Electronic Supplementary Material (ESI) for RSC Advances.

Photo and redox-responsive vesicles assembled from Bola-Type superamphiphiles

Tao Sun,[a] Lan Shu,[a] Jian Shen,[b] Chunhui Ruan,[a] Zhifeng Zhao,[a] Chen Jiang*[a]

[a]Key Laboratory of Smart Drug Delivery (Ministry of Education), State Key Laboratory of Medical Neurobiology, Department of Pharmaceutics, School of Pharmacy, Fudan University, Shanghai 201203, PR China

[b]School of Chemistry and Chemical Engineering, Weifang University, Weifang 261061, PR China

Supporting Information

Table of Contents

1. Characterizations of all compounds

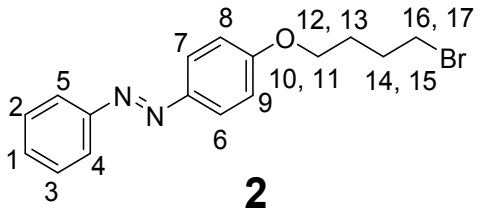

2

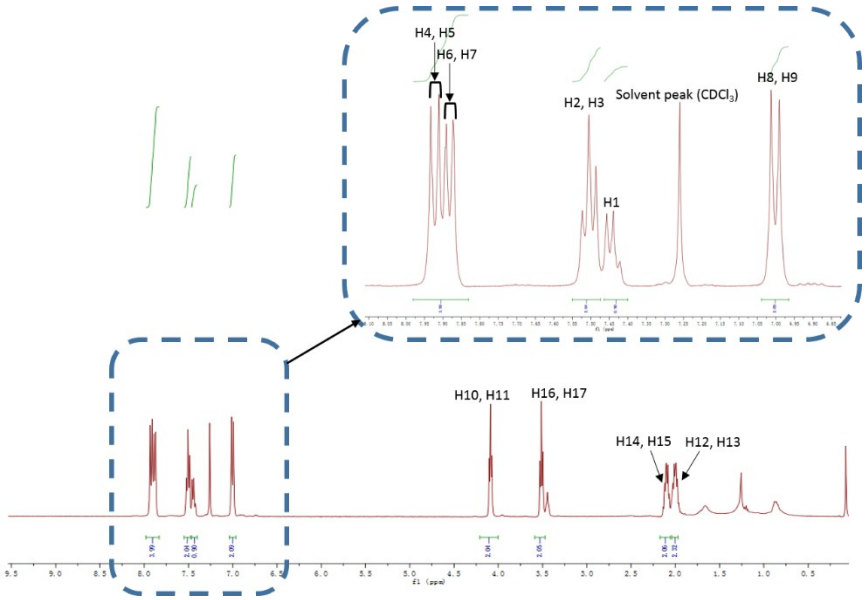

Figure S1. ^{1}H NMR spectrum of **2** in $CDCl_3$ at ambient temperature.

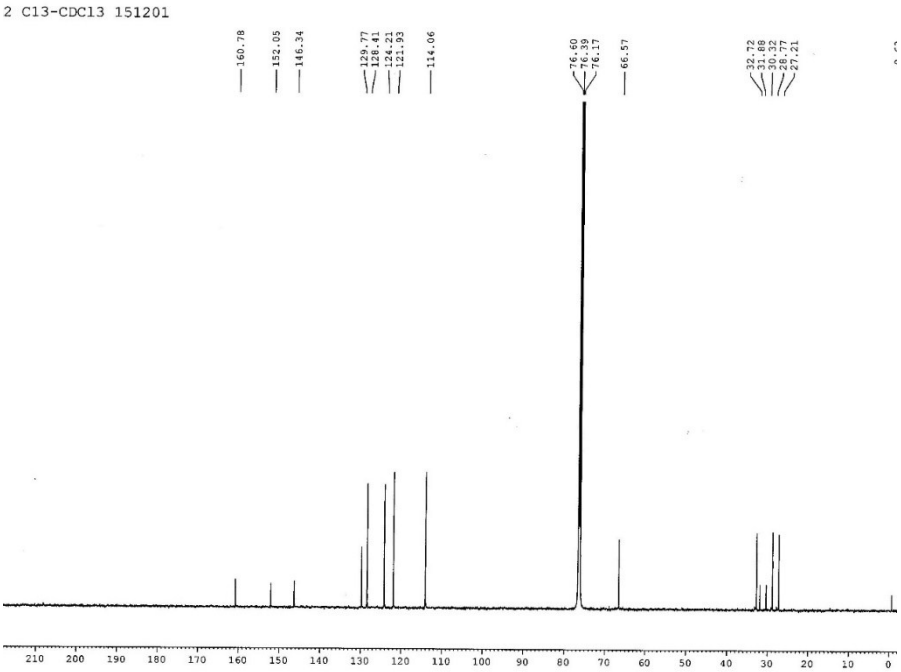

Figure S2. ^{13}C NMR spectrum of **2** in $CDCl_3$ at ambient temperature.

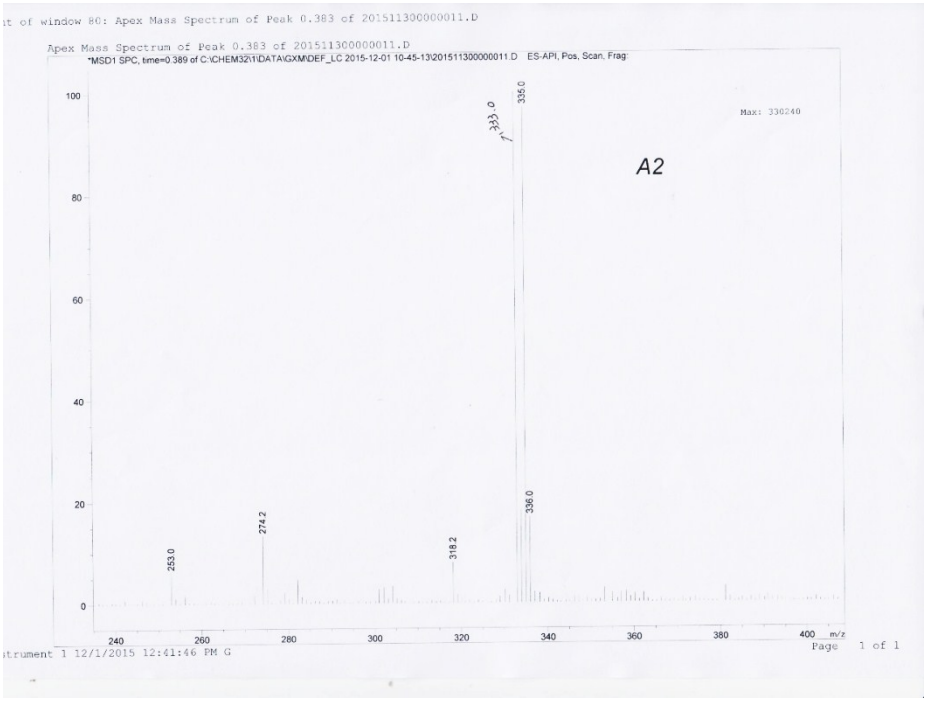

Figure S3. MS-ESI spectrum of **2** in $CDCl_3$ at ambient temperature.

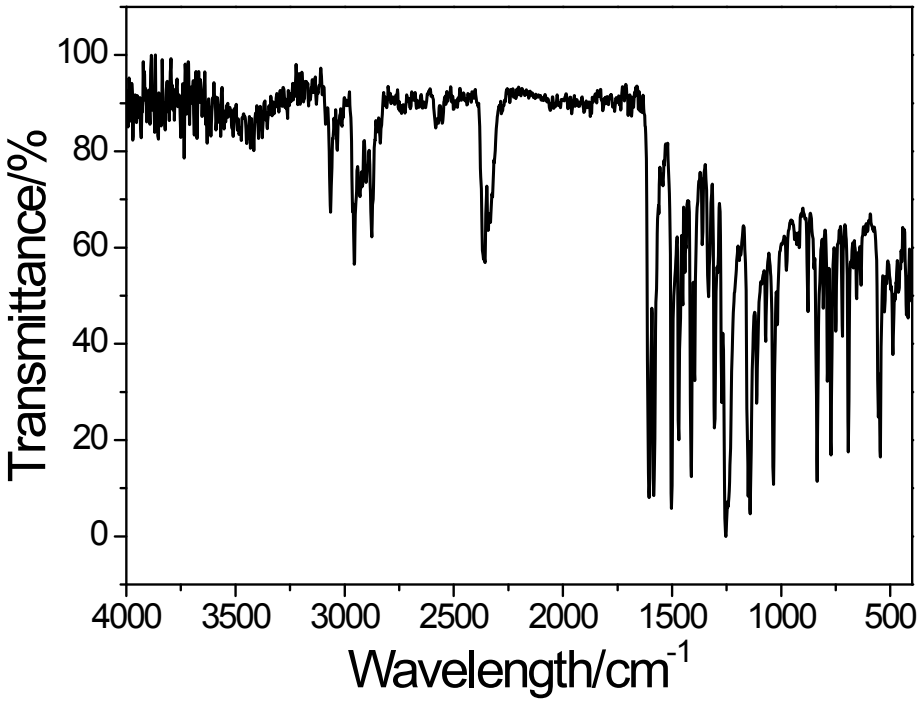

Figure S4. FT-IR spectrum of **3** in KBr tablet at ambient temperature.

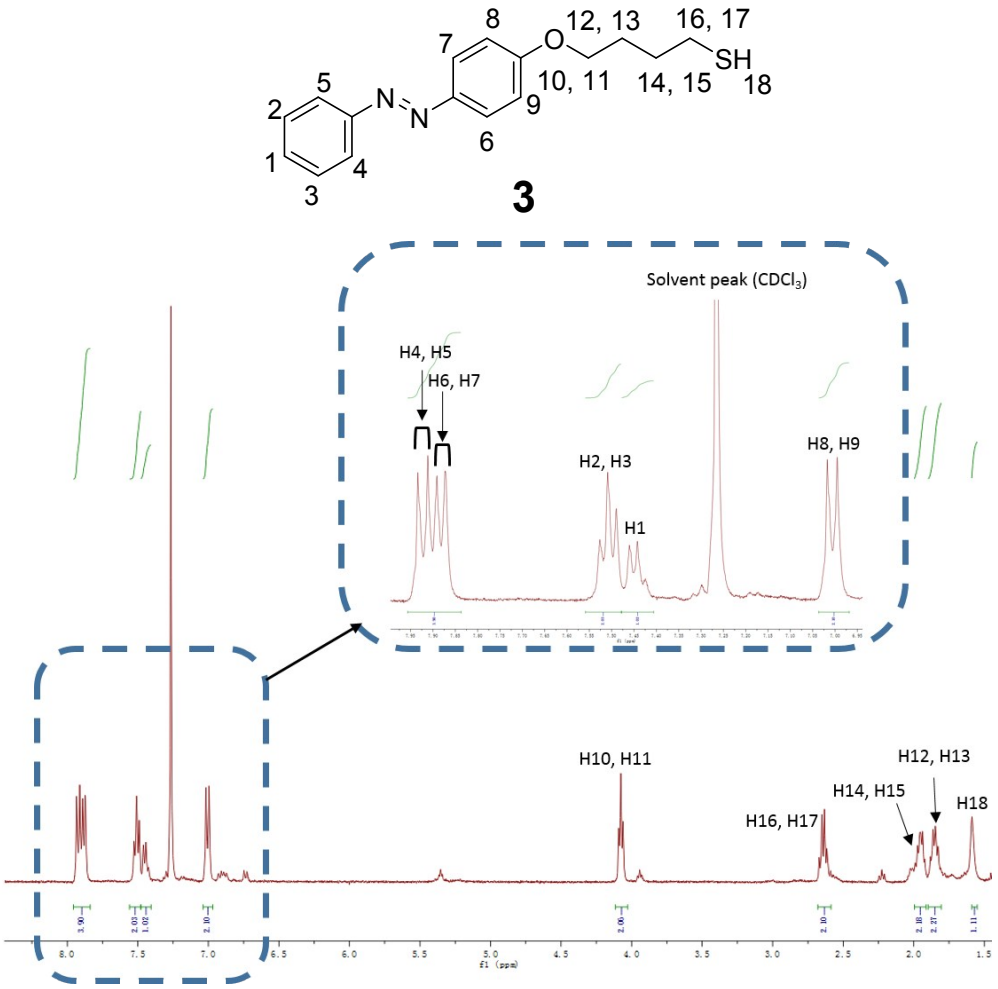

Figure S5. ^{1}H NMR spectrum of **3** in $CDCl_3$ at ambient temperature.

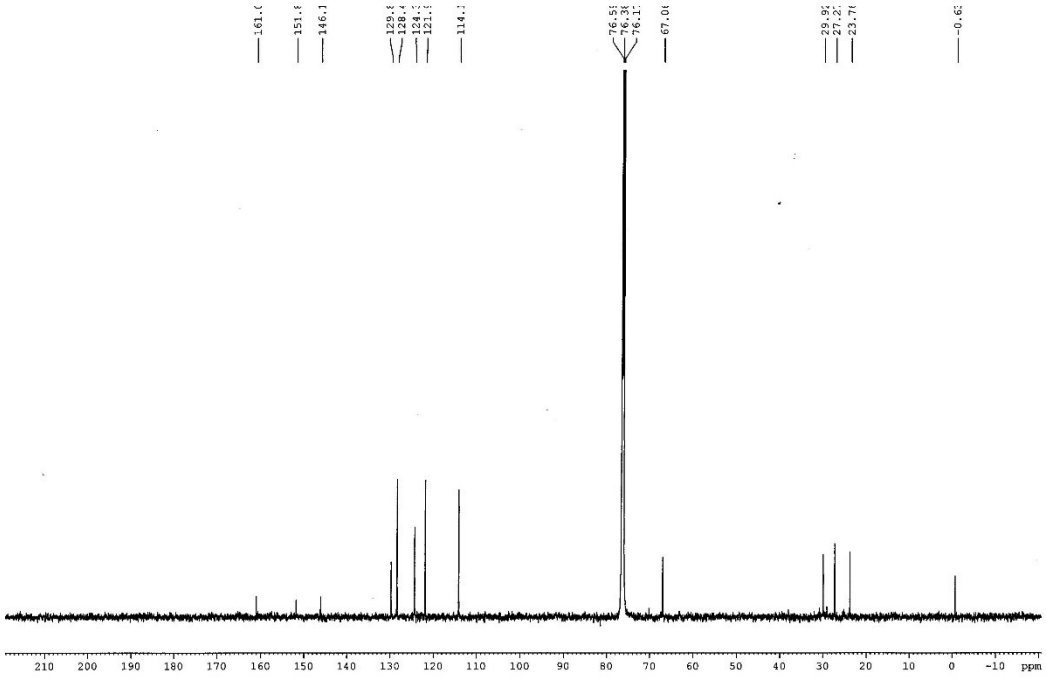

Figure S6. ^{13}C NMR spectrum of **3** in $CDCl_3$ at ambient temperature.

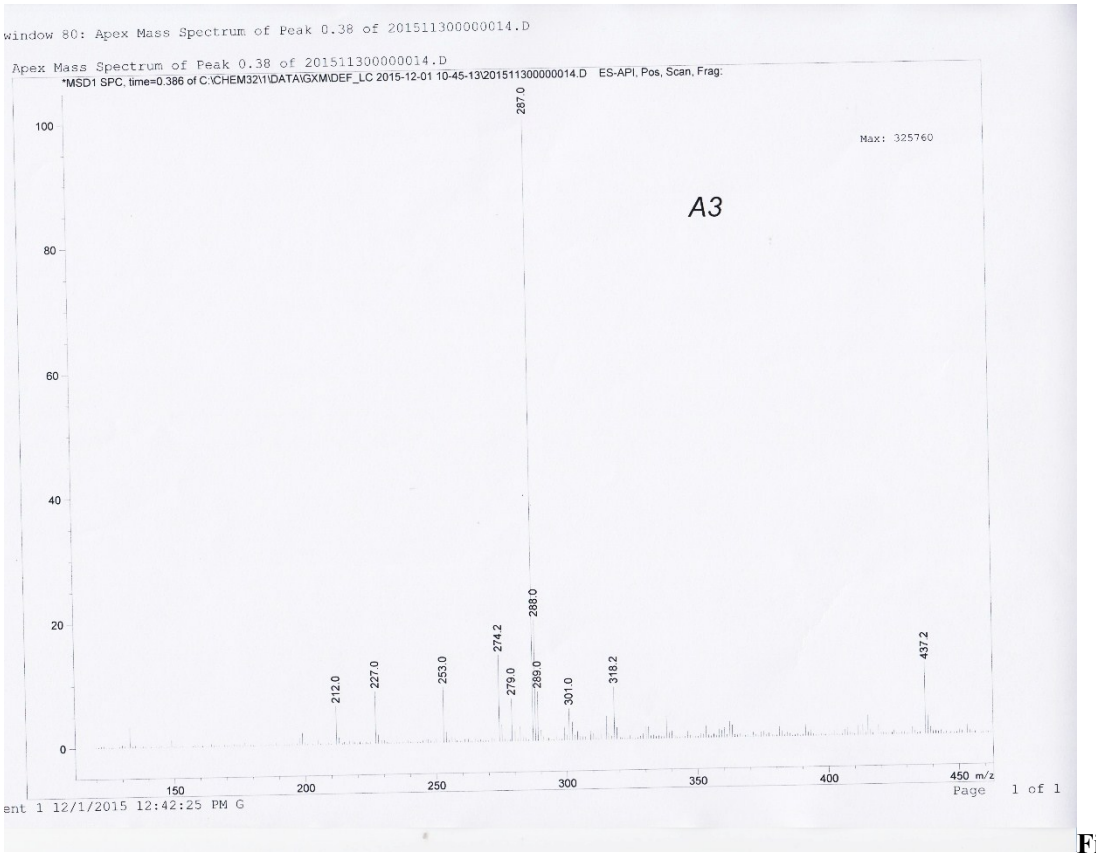

Figure S7. MS-ESI spectrum of **3** in $CDCl_3$ at ambient temperature.

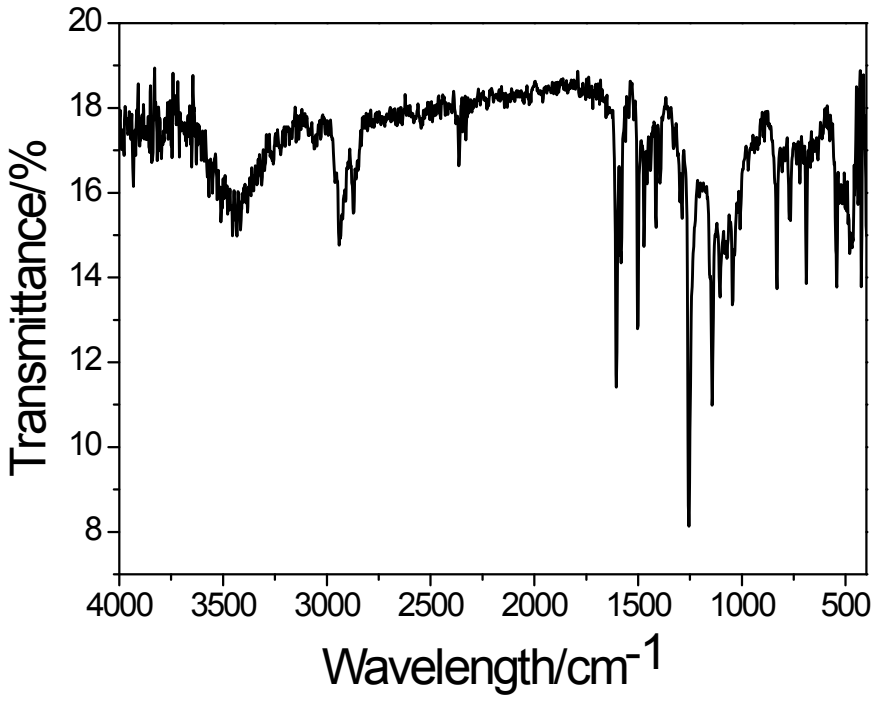

Figure S8. FT-IR spectrum of **3** in KBr tablet at ambient temperature.

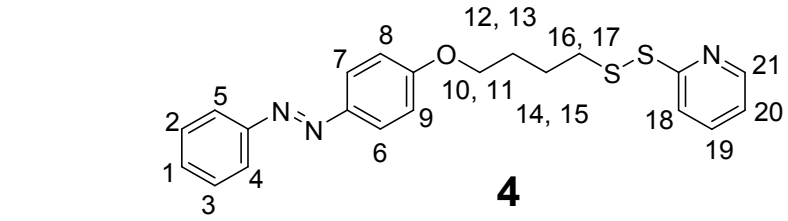

4

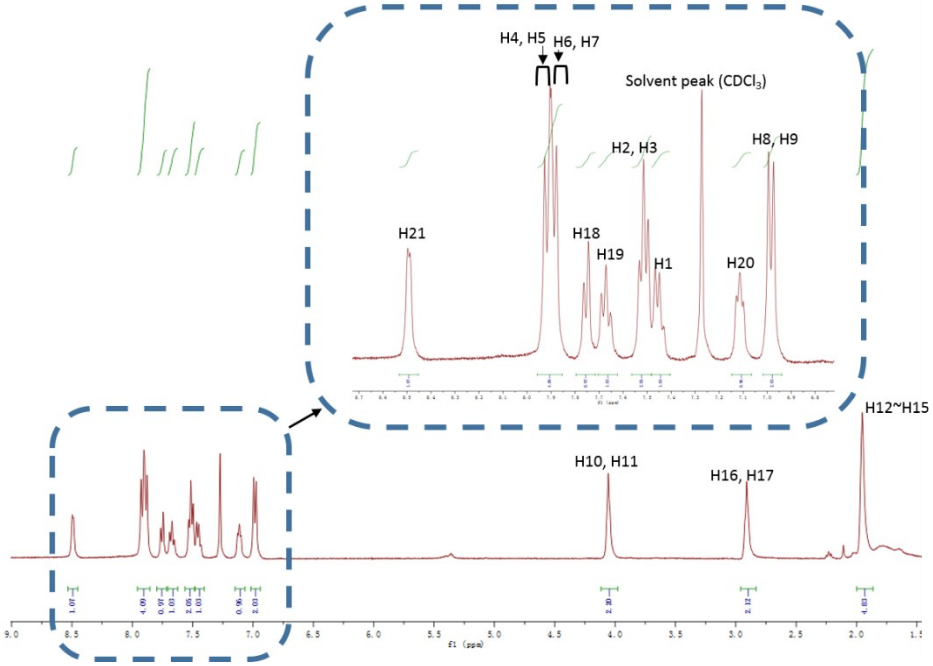

Figure S9. ^{1}H NMR spectrum of **4** in $CDCl_3$ at ambient temperature.

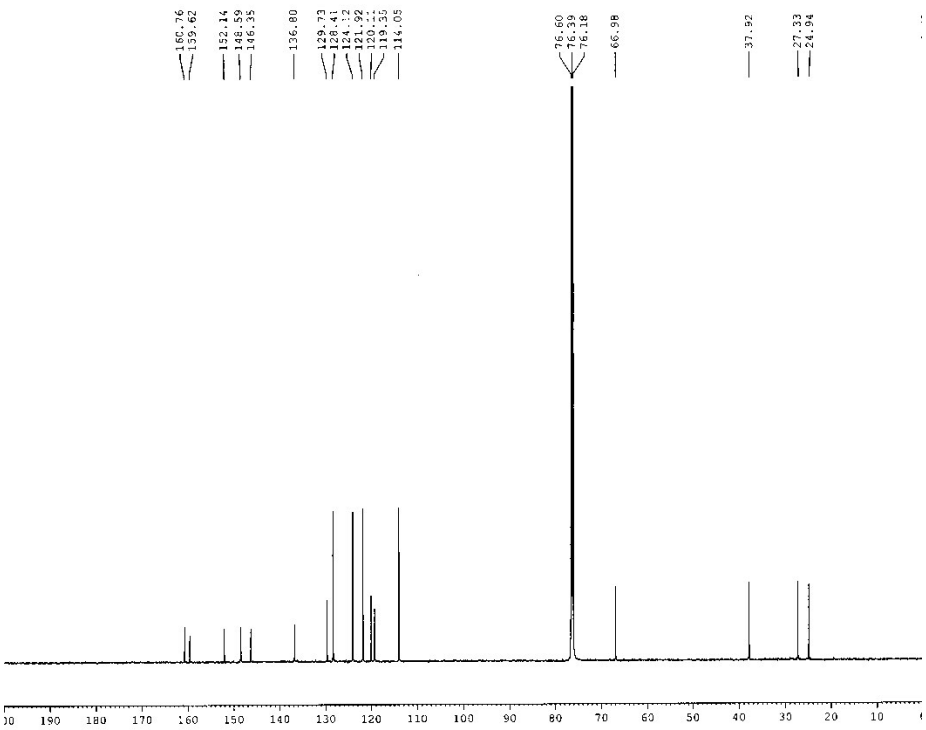

Figure S10. ^{13}C NMR spectrum of **4** in $CDCl_3$ at ambient temperature.

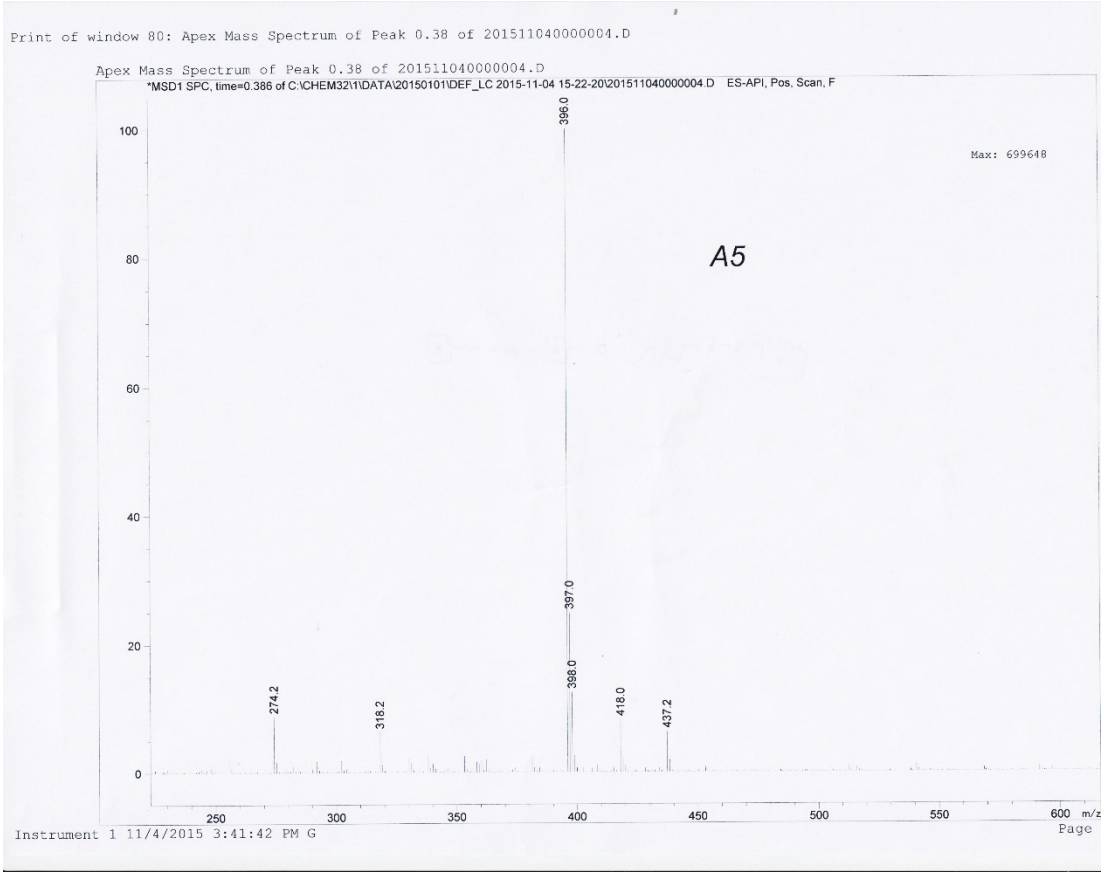

Figure S11. MS-ESI spectrum of **4** in $CDCl_3$ at ambient temperature.

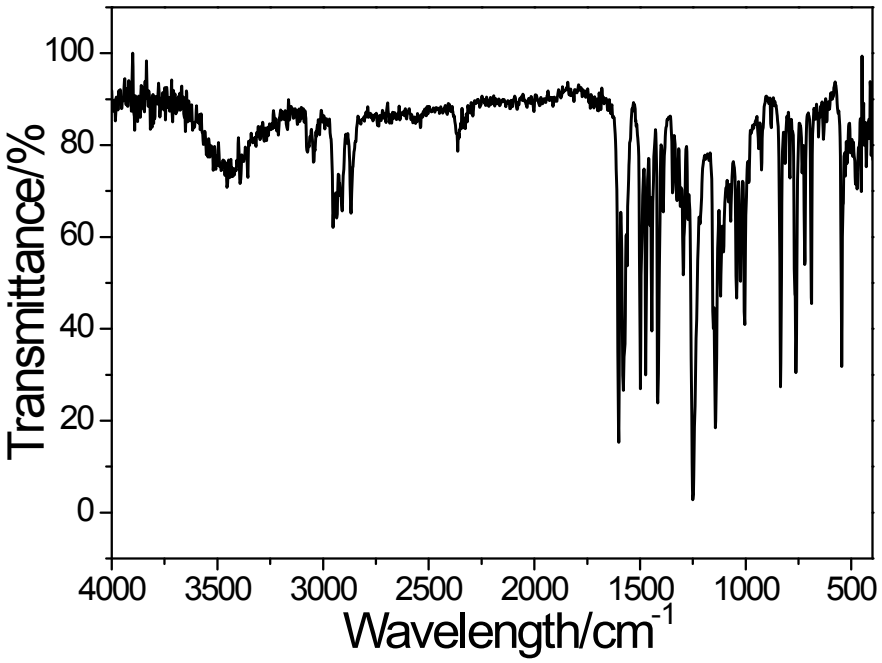

Figure S12. FT-IR spectrum of **4** in KBr tablet at ambient temperature.

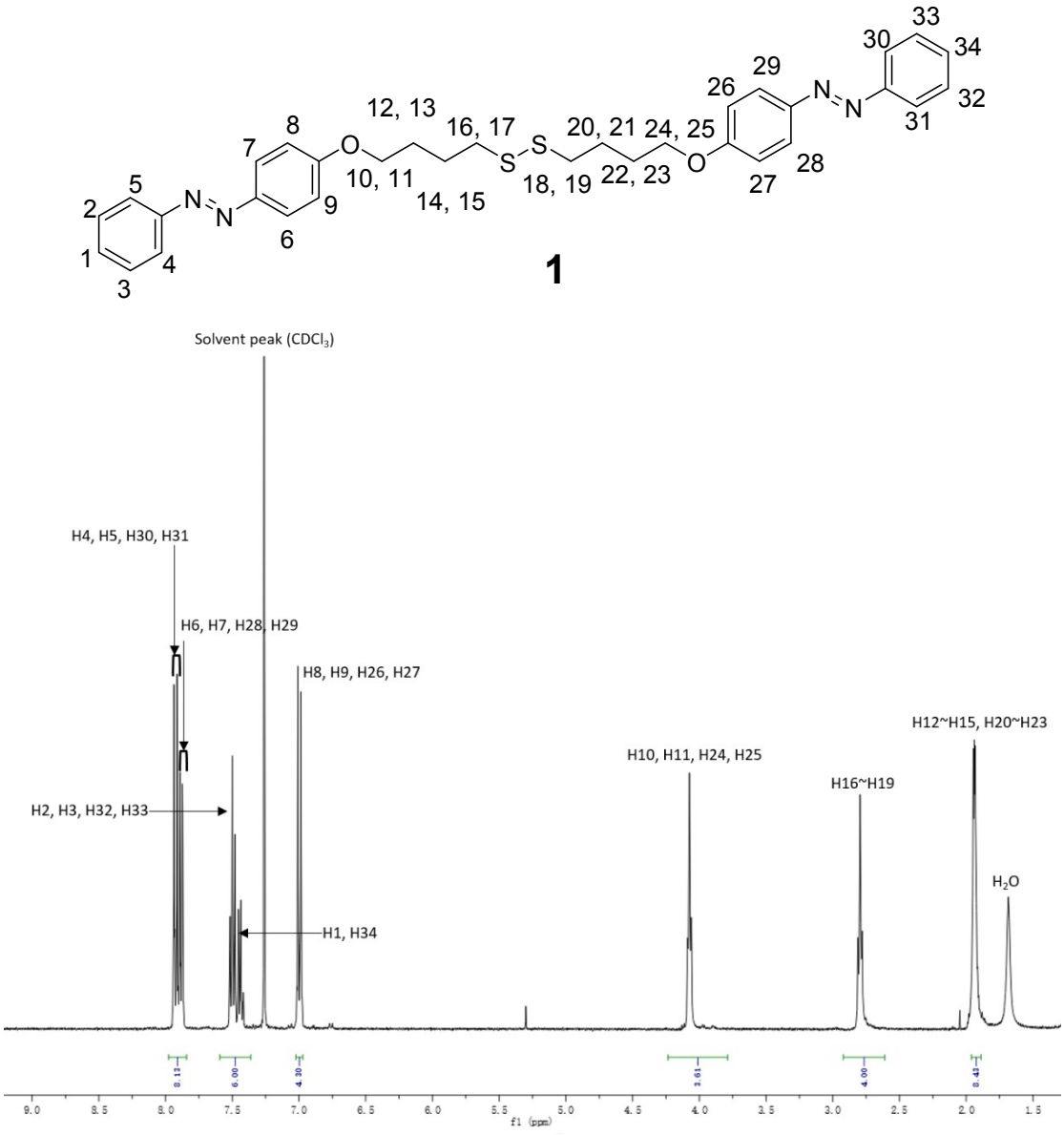

Figure S13. ^{1}H NMR spectrum of **1** in $CDCl_3$ at ambient temperature.

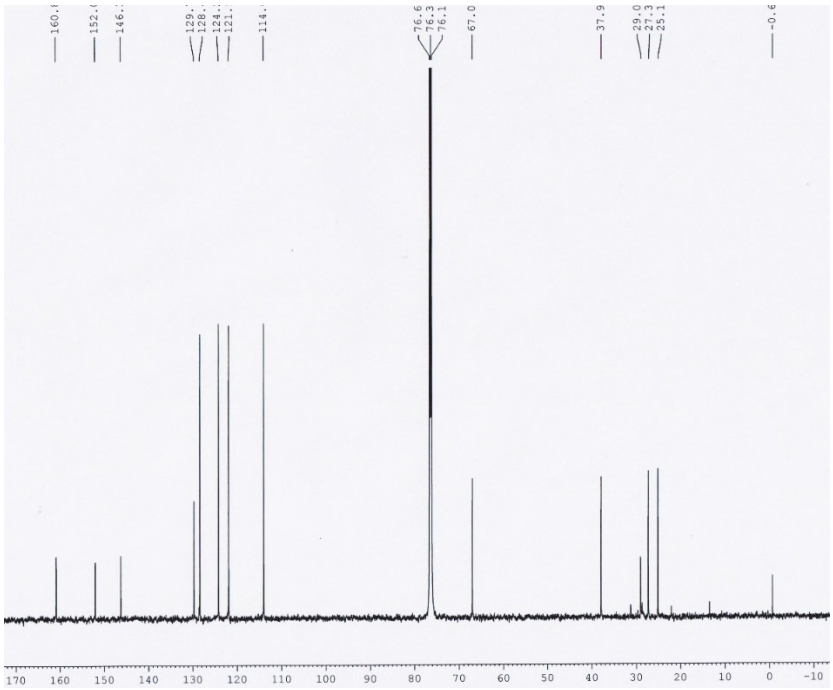

Figure S14. ^{13}C NMR spectrum of **1** in $CDCl_3$ at ambient temperature.

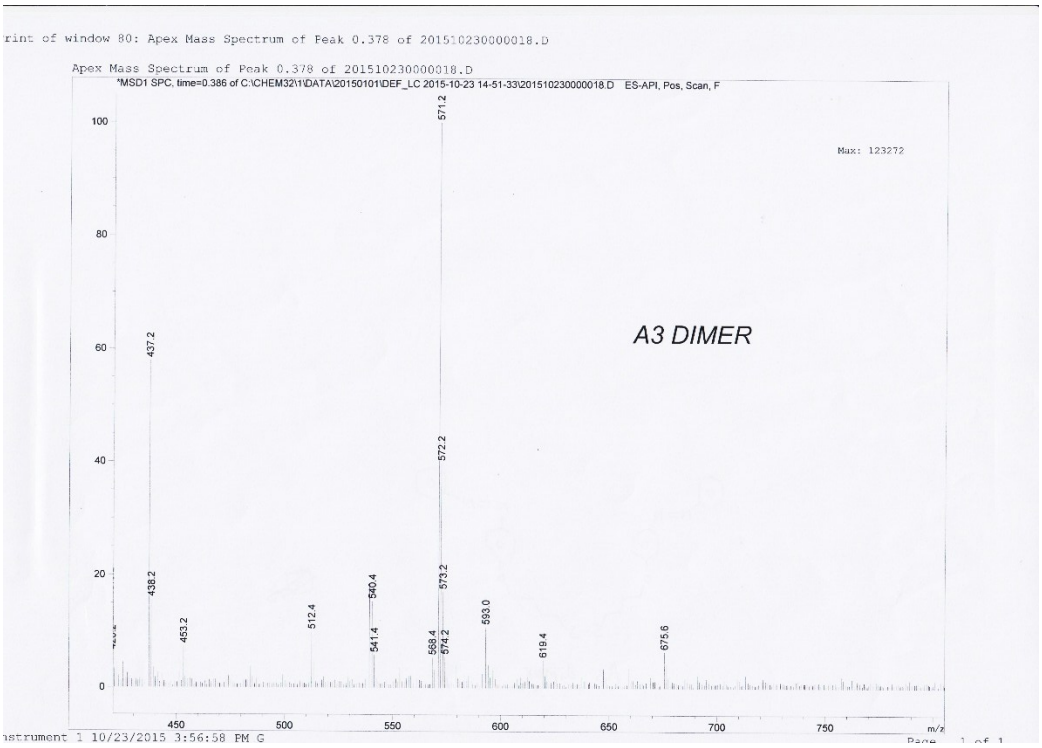

Figure S15. MS-ESI spectrum of **1** in $CDCl_3$ at ambient temperature.

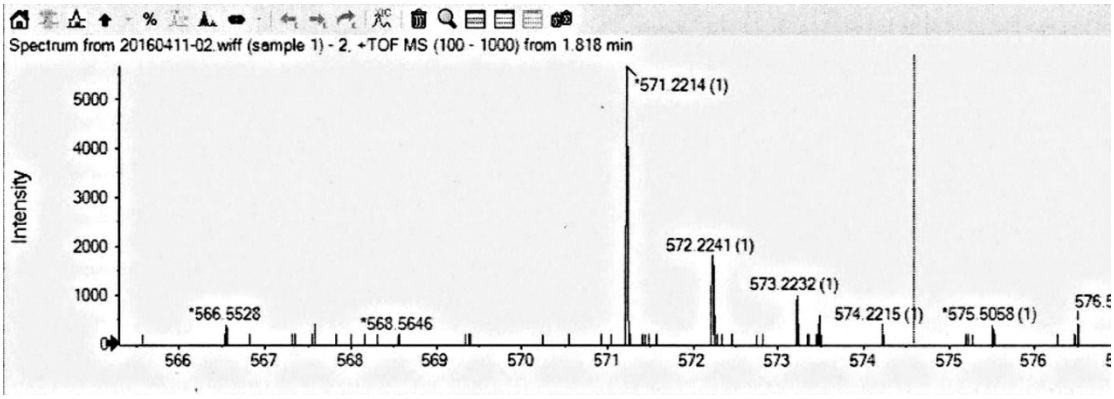

Figure S16. HR-Ms result of **1** at ambient temperature.

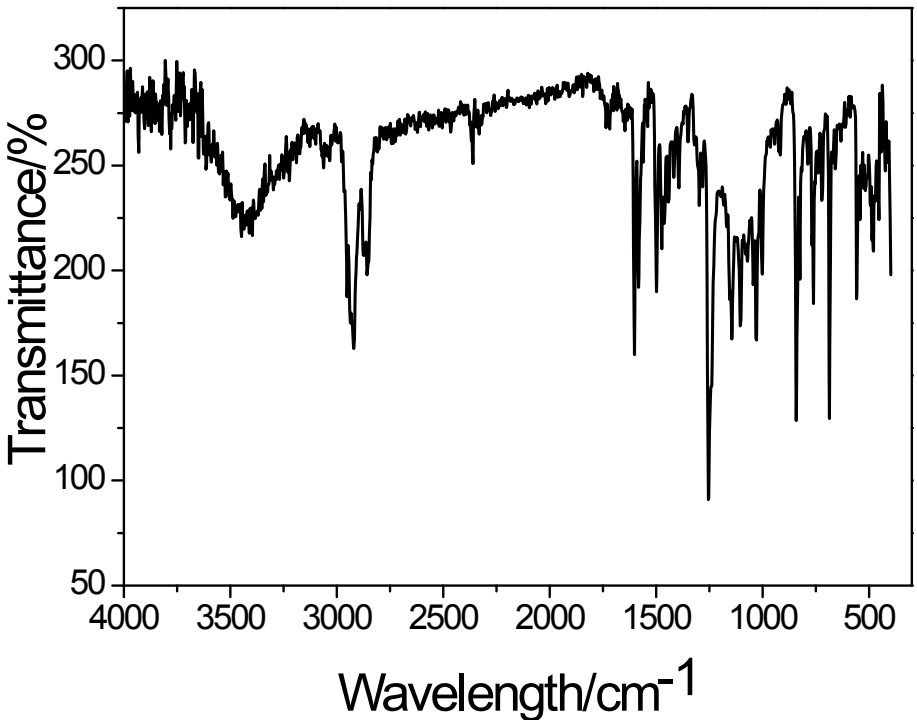

Figure S17. FT-IR spectrum of **1** in KBr tablet at ambient temperature.

2. Supporting information for the mechanism study

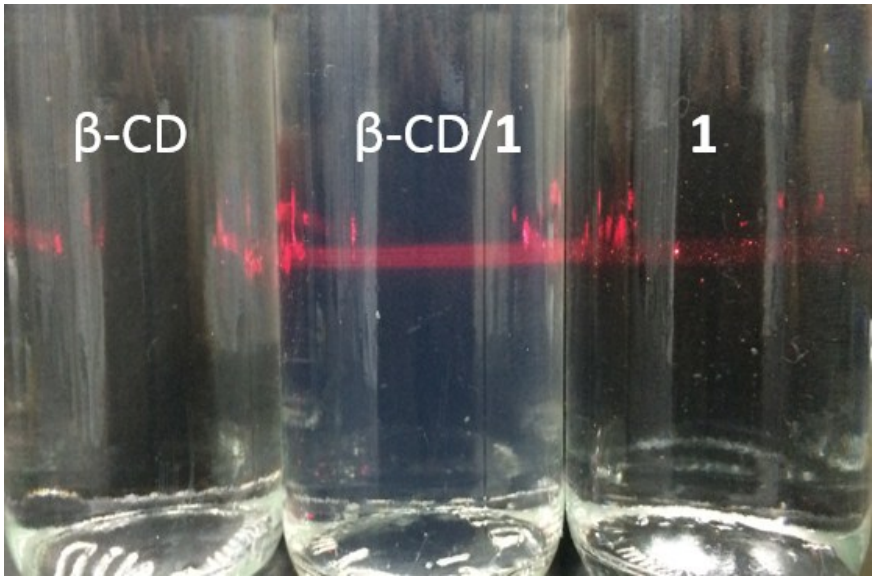

Figure S18. Different phenomenon of β-CD in aqueous solution (0.1 mM), β-CD/**1** vesicular solution (0.1 mM) and **1** aqueous dispersion in water (0.1 mM) illuminated by a laser pointer.

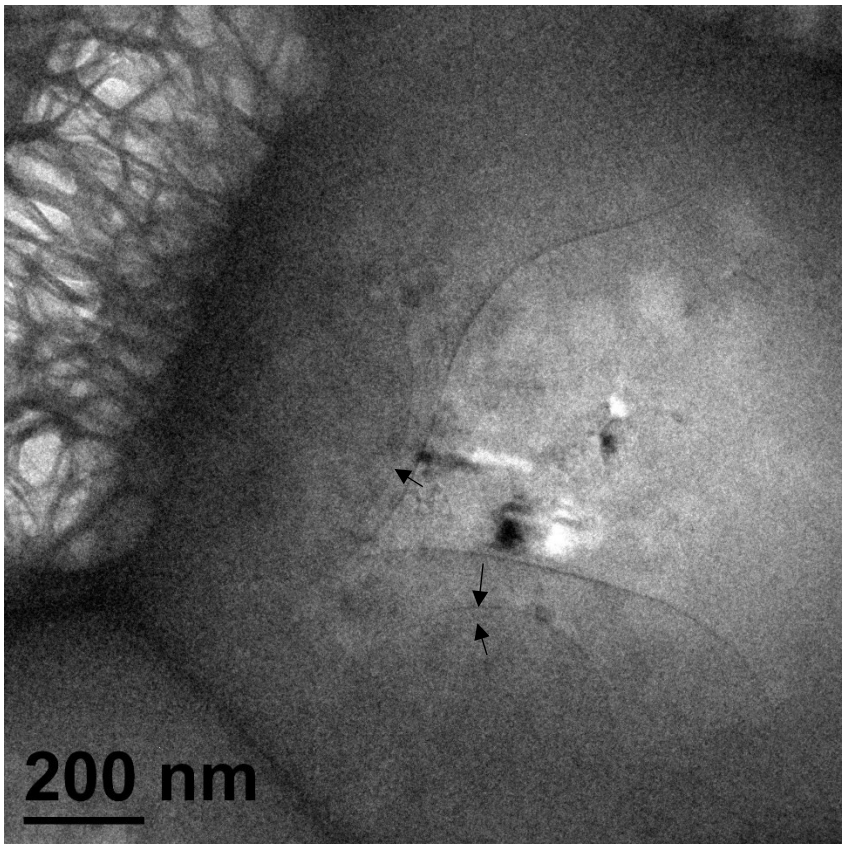

Figure S19. *Cryo*-TEM images of β-CD/**1** vesicular sample in water.

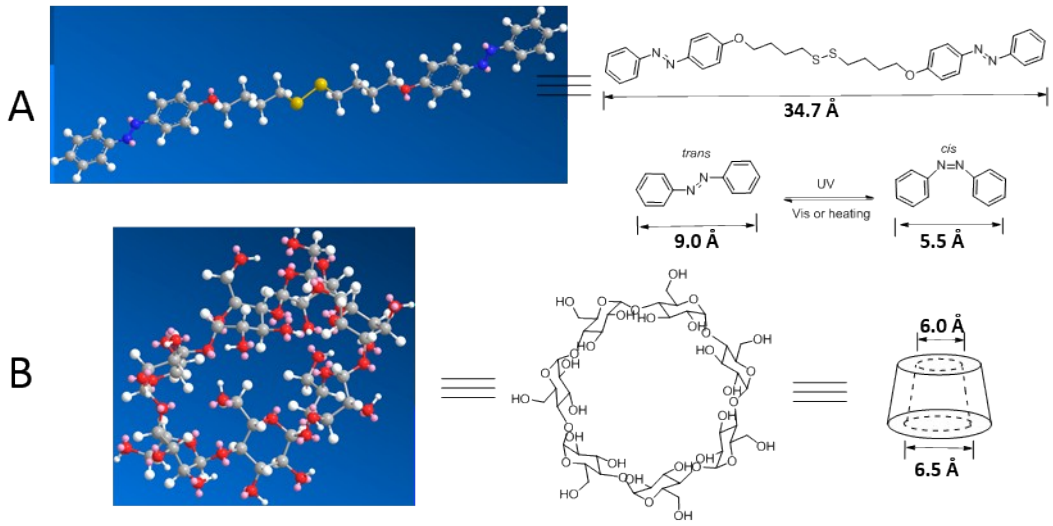

Figure S20. The molecular status after MM2 energy minimize calculation and corresponding calculated molecular sizes.[1]

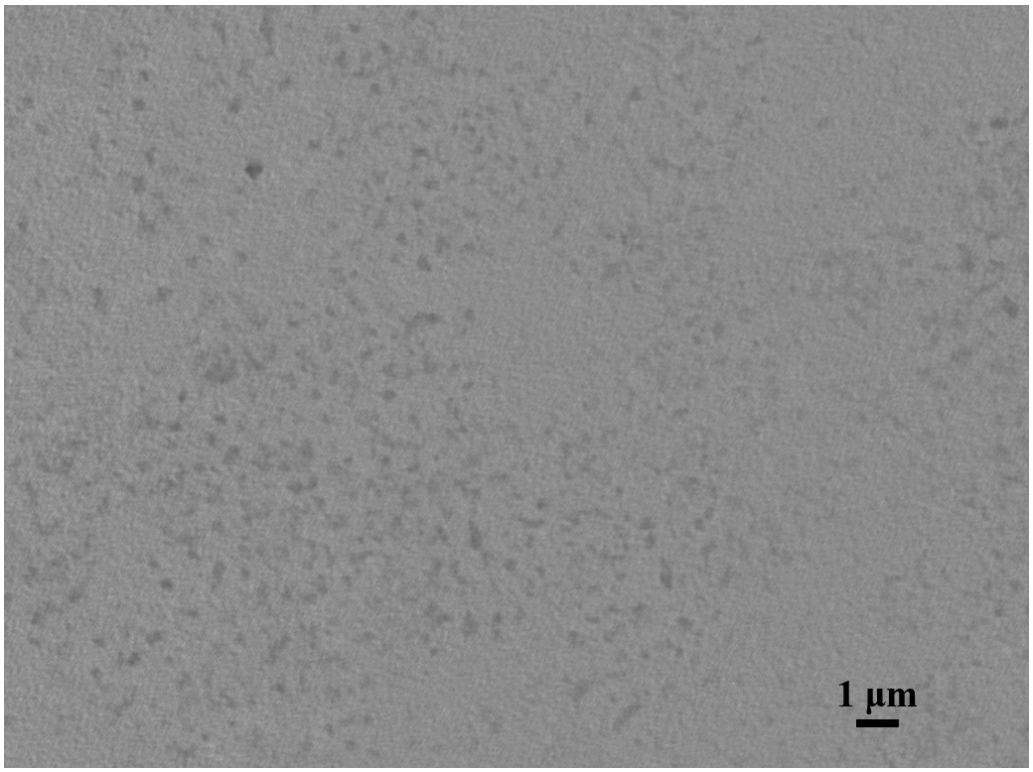

Figure S21. TEM micromorphology images of only β-CD in water after a 20 min sonication. Phosphotungstic acid was employed as the negative staining agent.

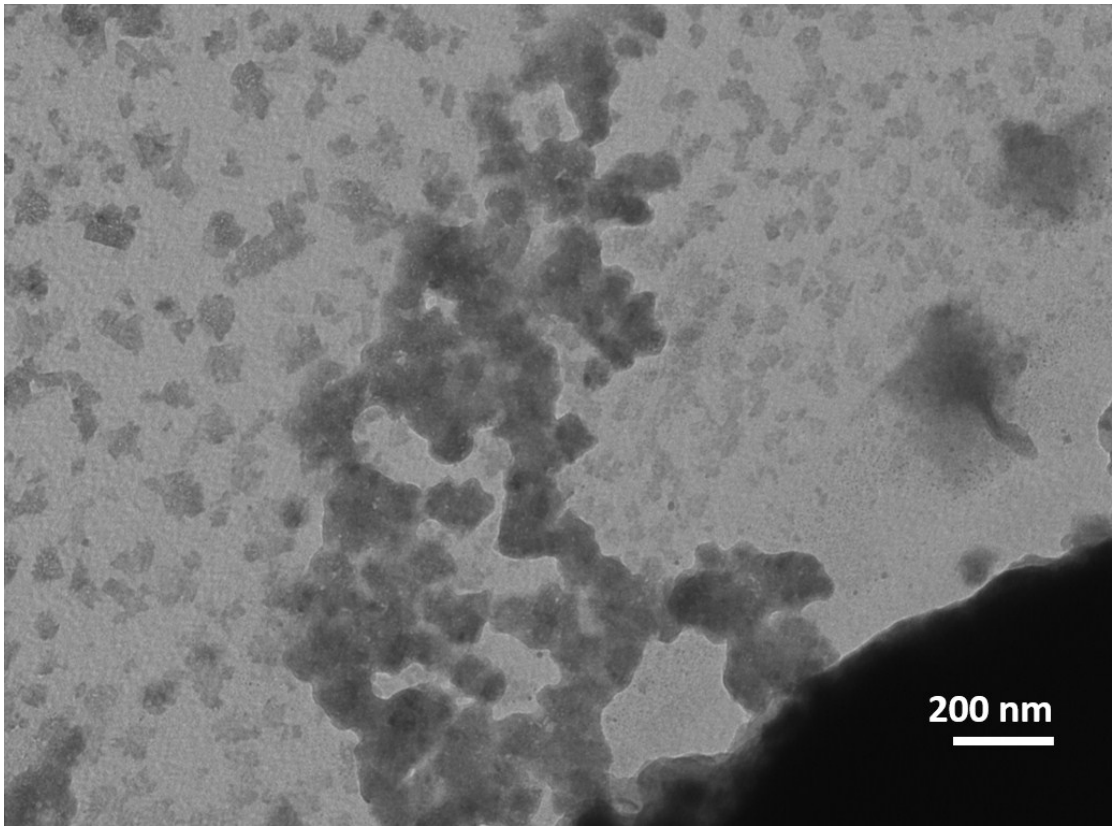

Figure S22. TEM micromorphology images of only compound **1** in water after a 20 min sonication. Phosphotungstic acid was employed as the negative staining agent.

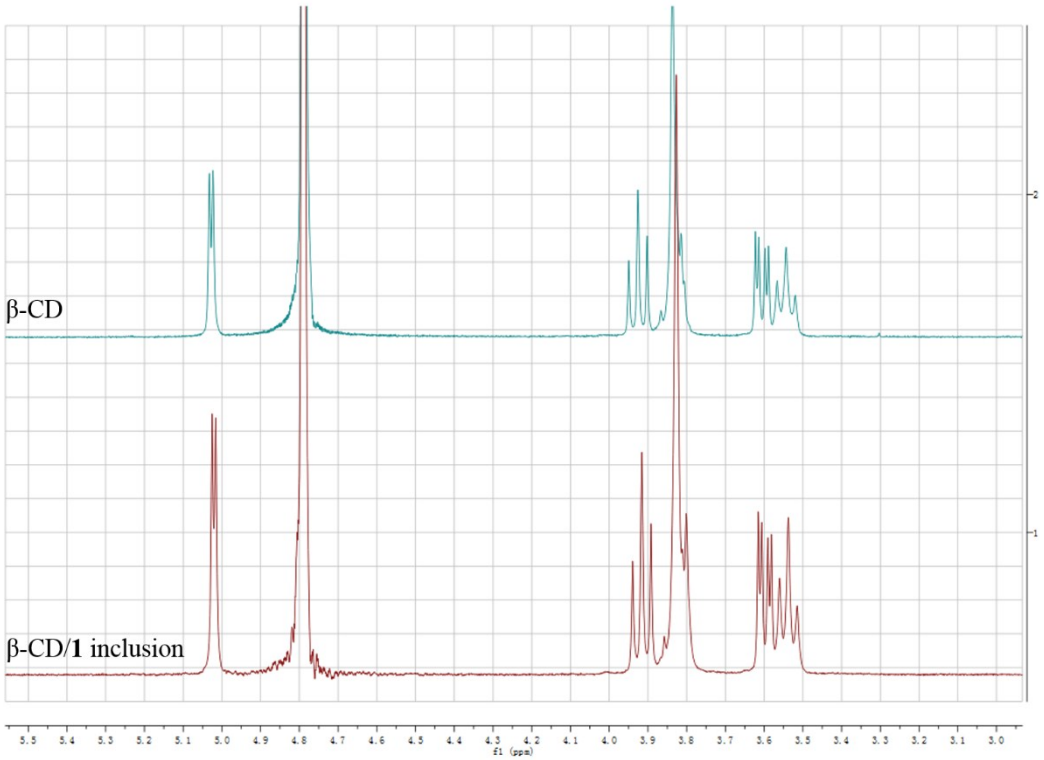

Figure S23. ^{1}H NMR spectra of β-CD and β-CD/**1** in D_2O at ambient temperature.

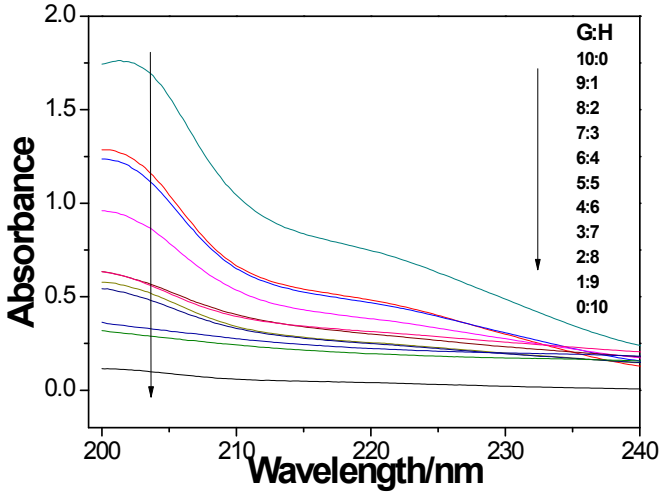

Figure S24. UV/vis spectra of **1**/β-CD (G/H = 10:0, 9:1, 8:2, 7:3, 6:4, 5:, 4:6, 3:7, 2:8, 1:9, 0:10, shown from top to down) for Job's plots in water at room temperature.

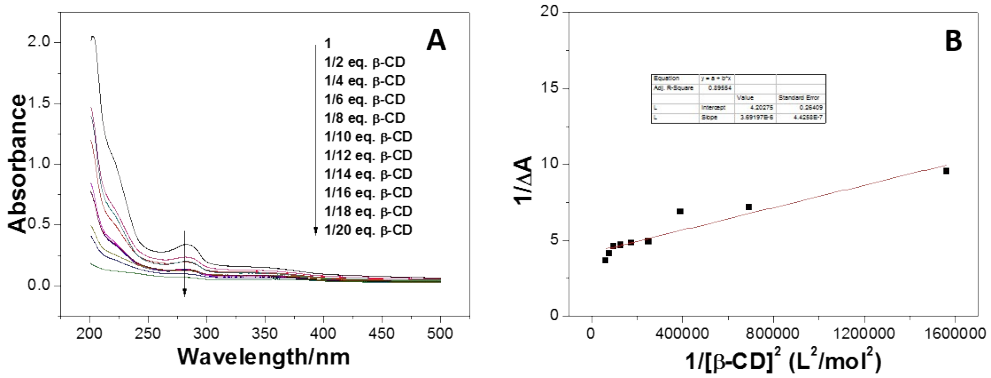

Figure S25. Double reciprocal plots of **1**/β-CD inclusion complex in water at 282 nm: (A) UV absorbance of **1** in presence of β-CD with different concentrations; (B) the complex constant calculated in 1:2 mode (G/H, $r^2 = 0.90$).

3. Photo- and redox-responsive properties

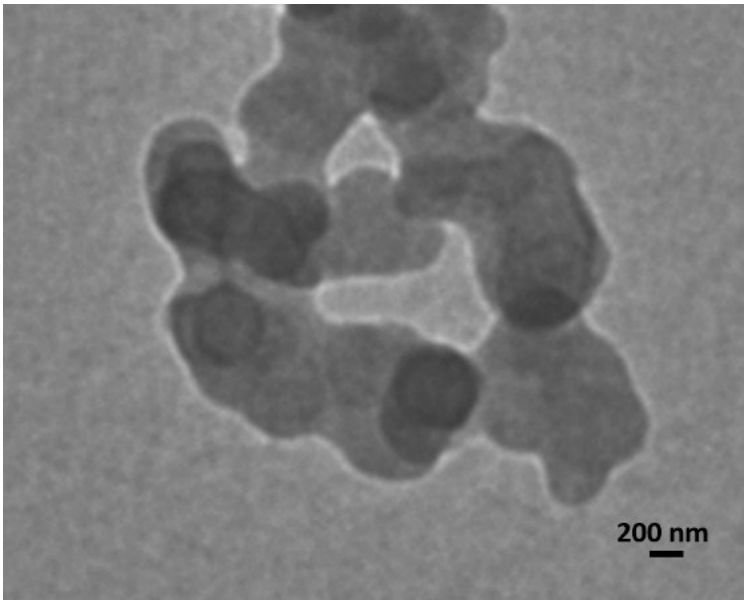

Figure S26. TEM micromorphology images of β-CD/**1** vesicular sample in water upon recovery with visible light irradiation. Phosphotungstic acid was employed as the negative staining agent.

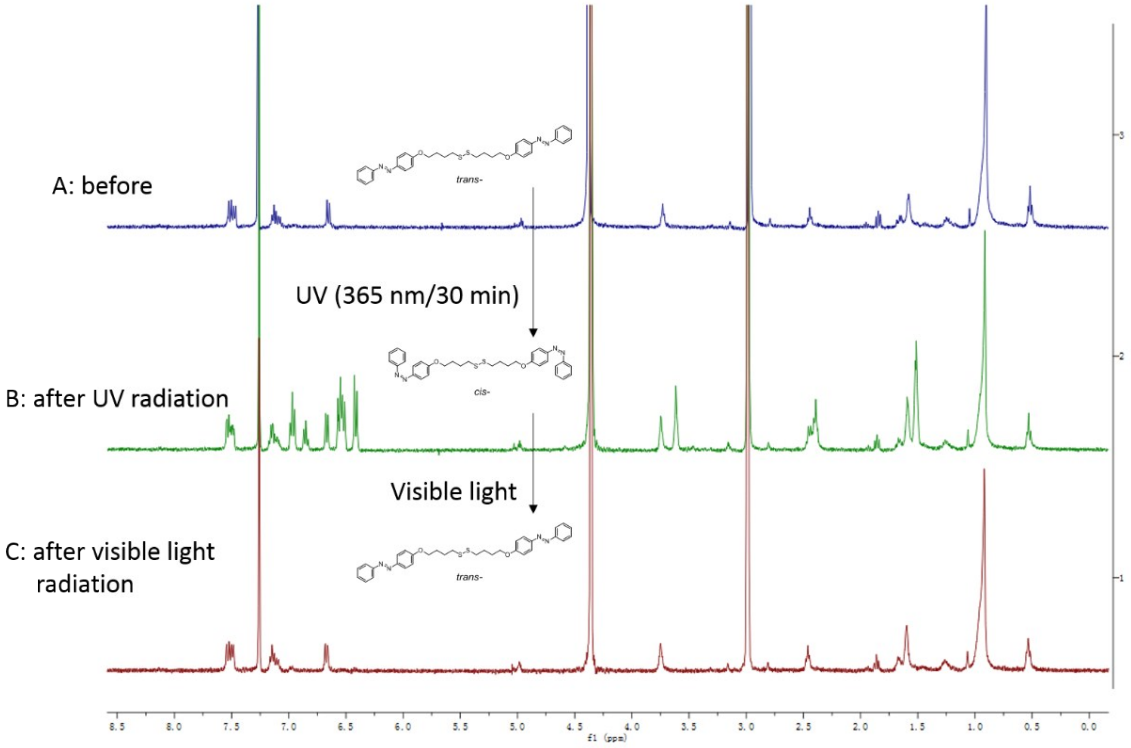

Figure S27. ^{1}H NMR spectra (400 MHz in $CD_3OD/CDCl_3$ (2/1, v/v) at 298 K, the entire version)

from the same tube of **1** before (A), after (B) UV irradiation (365 nm, 60 mW·cm^{-2}, 30 min) and (C) visible light radiation (434 nm, 20 mW·cm^{-2}, 5 h).

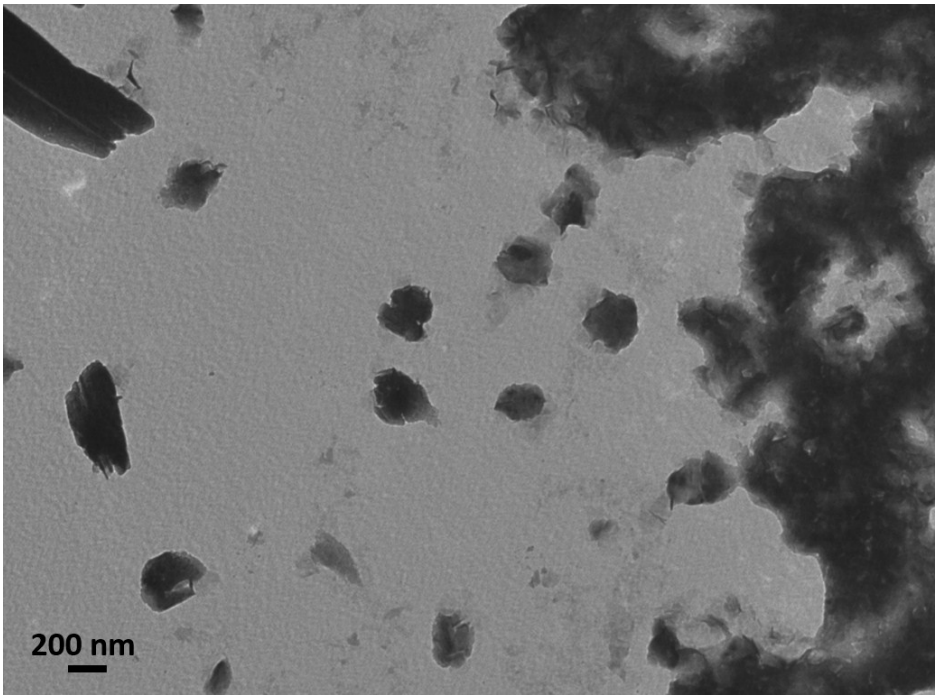

Figure S28. TEM micromorphology images of only β-CD/**1** sample in water upon DTT treatment. Phosphotungstic acid was employed as the negative staining agent.

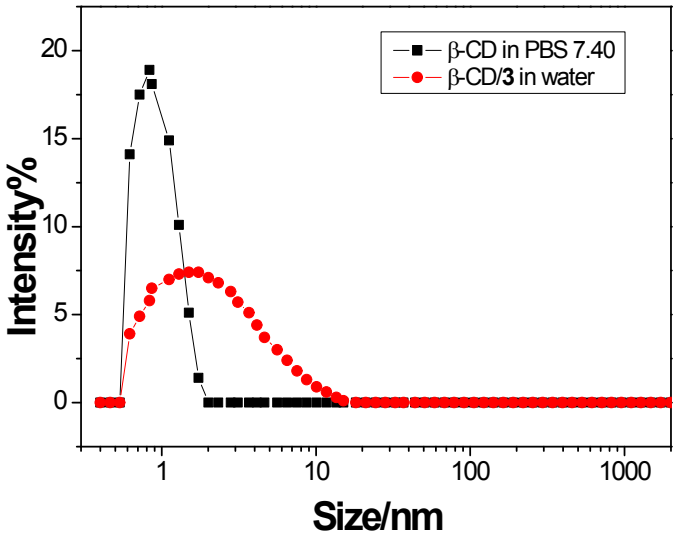

Figure S29. DLS results of the β-CD in PBS 7.40 (black, average size: 0.8 nm) and β-CD/**3** (red, average size: 1.8 nm) in water at 300 K.

4. Drug loading and release

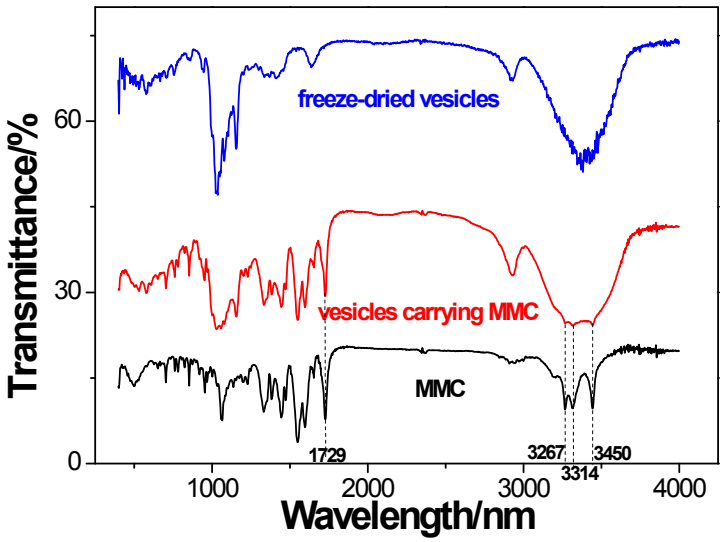

Figure S30. FT-IR spectra comparison of β-CD/**1** dried vesicles, and dried vesicles carrying mitomycin C (MMC) in KBr capsules at 300 K.

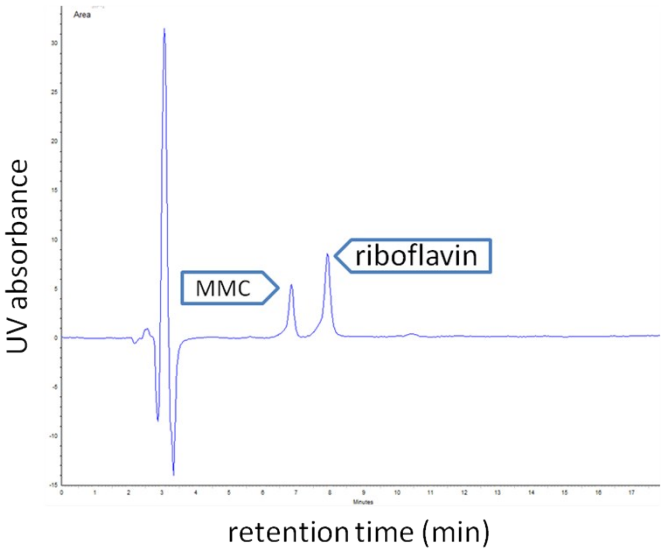

Figure S31. Representative HPLC chromatogram of MMC and riboflavin (internal standard)

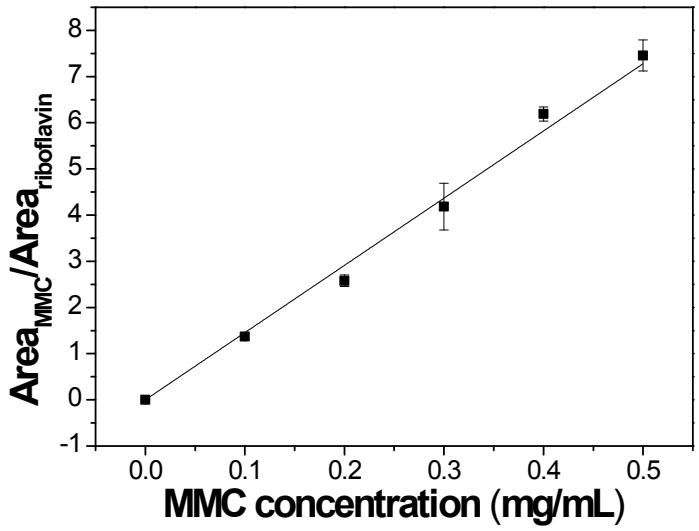

Figure S32. The standard curve of MMC concentration with riboflavin as the internal standard determined by HPLC. R^2=0.99393 and the values are represented as a mean ± SD (n = 3).

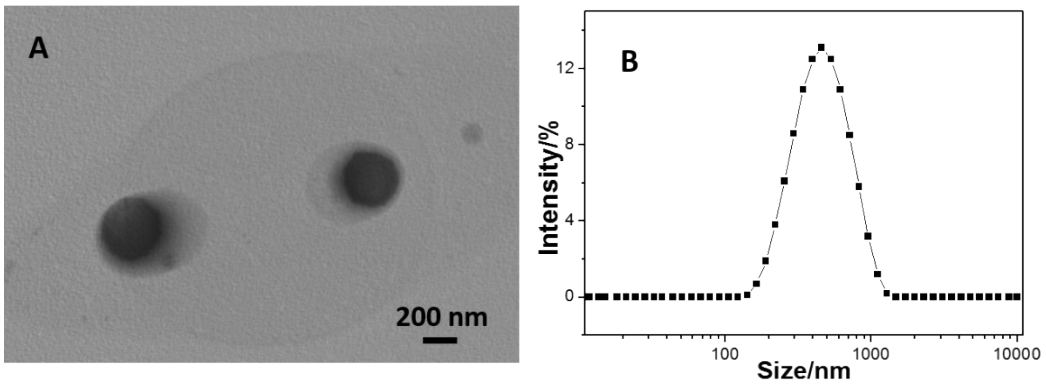

Figure S33. A: TEM micromorphology images (A) and DLS result (B) of pyrene-loaded β-CD/**1**/ vesicles in water. Phosphotungstic acid was employed as the negative staining agent.

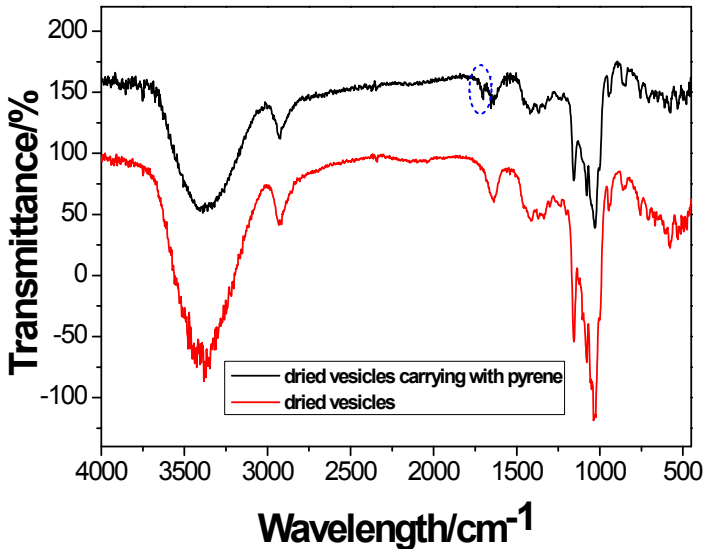

Figure S34. FT-IR spectra comparison of β-CD/**1** dried vesicles, and dried vesicles carrying pyrene in KBr capsules at 300 K.

Pyrene, with poor aqueous solubility (~10^{-6} mol/L) and high stability, can play the role as the hydrophobic drug model for the drug-carrying qualification.[2] We found that upon the drug loading, the β-CD/**1** vesicles' diameter tend to increase from TEM and DLS observations (417 nm, Figure S31). This may be due to the insertion of hydrophobic models into the bilayers.[3] The characteristic $\nu_{c=c}$ peak (1702 cm^{-1}) of pyrene in the FTIR spectrum demonstrates the successful carrying of pyrene to the vesicular system (Figure S32).

5. References of supporting information

1. T. Sun, H. Yan, G. Liu, J. Hao, J. Su, S. Li, P. Xing, A. Hao, Strategy of directly employing paclitaxel to construct vesicles. *J. Phys. Chem. B*, 2012, **116**, 14628−14636.
2. S. Li, T. Sun, X. Yang, B. Wang, P. Xing, Y. Hou, J. Su and A. Hao, Light-responsive drug carrier vesicles assembled by cinnamicacid-based peptide, *Colloid. Polym. Sci.*, 2013, **291**, 2639−2646.
3. J. Zhang, X. Li, M. Yan, L. Qiu, Y. Jin, K. Zhu, Hydrogen bonding-induced transformation of network aggregates into vesicles-A potential method for the preparation of composite vesicles, *Macromol. Rapid Commun.*, 2007, **28 (6)**, 710−717.